MITSUBISHI ELECTRIC RESEARCH LABORATORIES
http://www.merl.com

# Feedrate Optimization for Freeform Milling Considering Constraints from the Feed Drive System and Process Mechanics

Erkorkmaz, K.; Layegh, S.E.; Lazoglu, I.; Erdim, H.

TR2013-128 August 2013

**Abstract**

This paper presents a new and comprehensive strategy for planning minimum cycle time tool trajectories subject to both machining process related constraints, and also limitations of the feed drive control system. The machining process is considered by computing the workpiece-tool engagement along the toolpath and setting local feed limits to maintain a specified resultant cutting force. The drive constraints are considered by limiting the velocity, acceleration, and jerk magnitudes commanded to each actuator. Feed profiling is realized with uninterrupted acceleration transitions, capable of spanning multiple toolpath segments. Effectiveness of the proposed strategy is demonstrated in sculptured surface machining experiments.

*CIRP Annals Manufacturing TGechnology*

Contents lists available at SciVerse ScienceDirect

CIRP Annals Manufacturing Technology

Journal homepage: www.elsevier.com/locate/cirp

# Feedrate optimization for freeform milling considering constraints from the feed drive system and process mechanics

Kaan Erkorkmaz[1] (2), S. Ehsan Layegh[2], Ismail Lazoglu[2] (2), Huseyin Erdim[3]

[1]Precision Controls Laboratory, University of Waterloo, Waterloo, ON, Canada
[2]Manufacturing and Automation Research Center, Koç University, Istanbul, Turkey
[3]Mitsubishi Electric Research Laboratories, 201 Broadway, Cambridge, MA, USA

This paper presents a new and comprehensive strategy for planning minimum cycle time tool trajectories subject to both machining process related constraints, and also limitations of the feed drive control system. The machining process is considered by computing the workpiece-tool engagement along the toolpath and setting local feed limits to maintain a specified resultant cutting force. The drive constraints are considered by limiting the velocity, acceleration, and jerk magnitudes commanded to each actuator. Feed profiling is realized with uninterrupted acceleration transitions, capable of spanning multiple toolpath segments. Effectiveness of the proposed strategy is demonstrated in sculptured surface machining experiments.

Optimization, Milling, Feed

## 1. Introduction

Productivity and part quality are often competing objectives in manufacturing. In freeform machining of aerospace, automotive, die and mold, and biomedical components, complex geometries need to be produced in minimum time and cost, while preserving the given dimensional accuracy and form integrity specifications. Thus, process planning requires attention to both the machining mechanics and also the machines' dynamic capabilities.

Significant amount of research has been dedicated to modeling and optimizing 3- and 5-axis milling operations from a cutting mechanics standpoint ([1][2] and [3][4]). A parallel stream of research has studied trajectory generation, with the aims to improve toolpath smoothness for better part quality [5][6][7], and reduce cycle time by optimizing the feed subject to kinematic and dynamic limits of the drives [8][9][10][11]. In recent years, these efforts have begun to merge, leading to Virtual Machining Systems (VMS) where the cutting mechanics and CNC response are considered jointly in process simulation and optimization [12][13][14]. For example, the comprehensive VMS proposed by Merdol and Altintas [13][14] enables the material removal rate to be maximized subject to a large number of cutting process constraints, while also considering the CNC's trajectory planning for linear and circular toolpaths which are interpolated using acceleration-bounded feed transitions within the NC blocks [15].

In our paper, building on the earlier works in VMS, the cutting process mechanics is integrated with a comprehensive trajectory planning algorithm that is more suitable for freeform milling. The algorithm generates B-spline toolpaths, and time-optimized acceleration- and jerk-bounded axis trajectories by modulating the feed across large numbers of NC blocks without any unwanted interruption. This proposed integration provides:

1. The ability to machine freeform parts correctly, in minimum time, and in first trial; due to mitigation of some of the major factors that cause tool overload and tolerance violation;
2. A transparent interface for process planning; where the tool and workpiece motion (hence, engagement conditions) can be calculated accurately throughout the program, rather than being implicitly computed in the CNC after-the-fact.

## 2. Cutting process model

One of the most critical issues in complex freeform ball end milling is finding the engagement region between the tool and workpiece. Since entrance and exit angles along the tool axis varies from one cutter location (CL) point to another, the precision of simulated cutting forces is highly dependent on the accuracy of the engagement modeling. Using a Parasolid kernel, a cutter-workpiece engagement (CWE) model has been developed to calculate the instantaneous engagement map at each CL point [4]. An illustration of 3D and 2D engagement zones for a freeform surface is shown in Fig. 1. After 3D modeling, a 2D map of the engagement zone is generated to calculate the entrance and exit angles along the cutter axis with respect to the cross feed direction. A mechanistic force model, using polar sampling (for improved accuracy around the ball end tip), has been developed to estimate the cutting forces at each CL point. Fig. 2 shows the cutting force components that can be estimated using Eq. (1) [4].

$$dF_r = K_{rc} dA_C + K_{re} dZ \quad , \quad dF_\psi = K_{\psi c} dA_C + K_{\psi e} dZ$$
$$dF_t = K_{tc} dA_C + K_{te} dZ \tag{1}$$

Above, $K_{rc}$, $K_{\psi c}$ and $K_{tc}$ are radial, axial, and tangential cutting force coefficients, $K_{re}$, $K_{\psi e}$ and $K_{te}$ are the cutting edge coefficients, respectively. $dA_c$ and $dZ$ indicate instantaneous chip load and integration thickness along the tool axis.

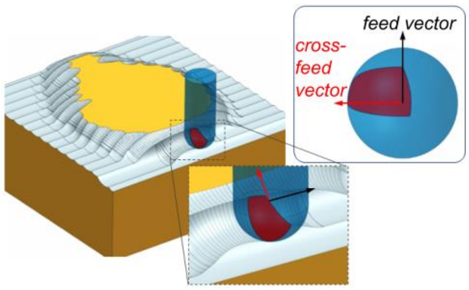


**Fig. 1.** Solid modeler based 2D CWE model.

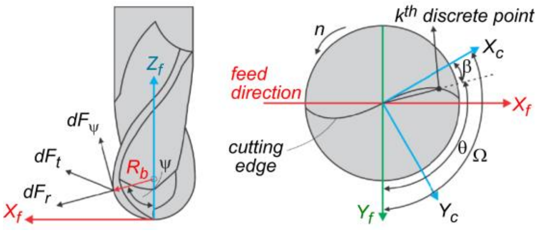


**Fig. 2.** Illustration of cutting force components.

For estimation of the instantaneous resultant cutting force, an appropriate transformation matrix is required to transfer the elemental forces from local coordinates to the measurement coordinate frame. By integrating the transformed elemental forces along the cutting edge for each flute, the instantaneous resultant force acting on the cutter is estimated [16].

The simulated and measured resultant forces for five toolpaths are shown in Fig. 3. These are for a two-flute ball end mill with 6 mm radius, cutting aerospace grade Aluminum alloy Al-7050 at a constant feedrate of 500 mm/min. As can be seen, at some instances there is discrepancy between the simulated and measured cutting force. This problem is due to the lack of CL points generated by the computer aided manufacturing (CAM) software, particularly at locations where the engagement changes considerably. This can be remedied by integrating the force simulation with trajectory planning inside a common platform.

In traditional milling operations, the feed is kept conservatively constant during machining, in order to avoid tool breakage, machine tool damage, dimensional errors, and so on. By estimating the engagement region and cutting forces at each CL point, and utilizing the near linear relationship between feedrate and resultant cutting force, a feed scheduling model has been developed, similar to the one in [2][13][14]. Using this model, the resultant cutting force is regulated around a specified limit $F_{\lim}$, so that when the engagement region is small, the feedrate is increased automatically, in order to shorten cycle time and boost productivity. As can be inferred from Eq. (1), any differential cutting force component $dF_j$ can be related to the feedrate $f$ as:

$$dF_j = Af + B \tag{2}$$

Above, $A$ and $B$ are constants. Eq. (2) applies for a wide range of rough and finish machining conditions, where ploughing is not a dominant deformation mechanism. The cutting force based feed limits are determined by running the process simulation at two different constant feed values ($f_1$ and $f_2$) and logging the resultant cutting force ($F_{1,i}$, $F_{2,i}$) at each CL point. Here, $F_{1,i}$ is the simulated resultant force at point $i$ for feed $f_1$, and $F_{2,i}$ for feed $f_2$. The feed limit at each point $i$ is then determined as:

$$f_{\lim,i} = (F_{\lim} - F_{1,i})(f_2 - f_1)/(F_{2,i} - F_{1,i}) + f_1 \tag{3}$$

Fig. 4 shows the feed limits generated by this strategy, in order to keep the resultant cutting force at 250 N. The scheduling was

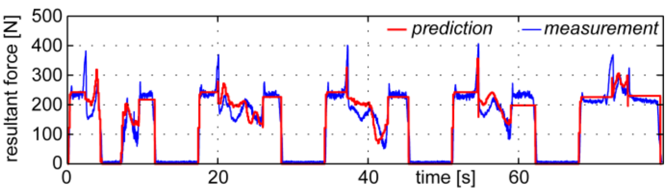


**Fig. 3.** Predicted and measured resultant cutting forces.

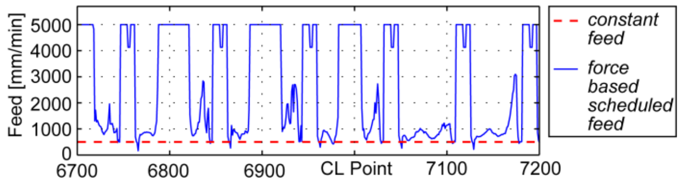


**Fig. 4.** Force based scheduled feedrate for each CL point.

computed after running two simulations, one for $f_1$ =500 mm/min, and the other for $f_2$ =1000 mm/min. 5000 mm/min was the maximum cutting feed limit set in the CNC.

## 3. Feed drive limits

The drive limits considered are axis velocity, acceleration, and jerk ($\dot{\boldsymbol{r}}_{\max}, \ddot{\boldsymbol{r}}_{\max}, \dddot{\boldsymbol{r}}_{\max}$). Limiting these helps preserve drive component life, avoid actuator saturation, and limit the dynamic positioning errors and structural vibrations [9]. Expressing the tool position $\boldsymbol{r} = \boldsymbol{r}(s(t))$ as a function of arc displacement ($s$) evolving over time ($t$), the commanded trajectory, at toolpath segment $k$, should satisfy:

$$\left.\begin{array}{l}
|\dot{\boldsymbol{r}}| = |\boldsymbol{r}_s \dot{s}| \leq |\boldsymbol{r}_s| f_k \leq \dot{\boldsymbol{r}}_{\max} \\
|\ddot{\boldsymbol{r}}| = |\boldsymbol{r}_{ss}\dot{s}^2 + \boldsymbol{r}_s \ddot{s}| \leq |\boldsymbol{r}_{ss}| f_k^2 + |\boldsymbol{r}_s| a \leq \ddot{\boldsymbol{r}}_{\max} \\
|\dddot{\boldsymbol{r}}| = |\boldsymbol{r}_{sss}\dot{s}^3 + 3\boldsymbol{r}_{ss}\dot{s}\ddot{s} + \boldsymbol{r}_s \dddot{s}| \leq \ldots \\
\qquad |\boldsymbol{r}_{sss}| f_k^3 + 3|\boldsymbol{r}_{ss}| a f_k + |\boldsymbol{r}_s| J \leq \dddot{\boldsymbol{r}}_{\max}
\end{array}\right\} \tag{4}$$

To ensure that a feasible feed limit $f_k$ can be found, the tangential acceleration and jerk magnitudes ($a$ and $J$) are set to,

$$\begin{array}{l}
a \leq A = \alpha_{acc} \min(\ddot{\boldsymbol{r}}_{\max}) \ , 0 < \alpha_{acc} < 1 \\
J = \alpha_{jerk} \min(\dddot{\boldsymbol{r}}_{\max}) \ , 0 < \alpha_{jerk} < 1
\end{array} \tag{5}$$

For efficiency, $f_k$ is solved using bisection while checking Eq. (4). Since the signs of tangential acceleration and jerk are not known ahead of time, there is some conservativeness caused by having to apply the triangle inequality (i.e., $|A+B| \leq |A| + |B|$). Nevertheless, this approach yields feed limits that are calculated efficiently, and obey the specified drive constraints while making reasonably good use of the drives' capabilities. When solving $f_k$, to further reduce cycle time, the envelope of possible acceleration magnitudes is considered, as shown in Fig. 5, for jerk limited motion within the achievable feed range of $[0, V]$.

## 4. Overall optimization scheme

The proposed optimization scheme, which integrates the cutting process model and feed drive limits, is shown in Fig. 6. The toolpath is planned in commercial CAM software as CL data (Fig. 6a). The CAM model and CL points are used to resolve the engagement geometry (Fig. 6b), which makes it possible to

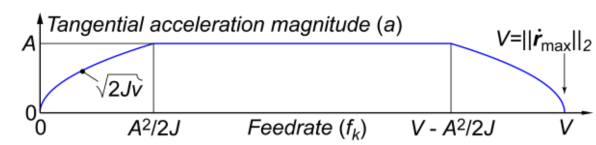


**Fig. 5.** Envelope of possible acceleration magnitudes for piecewise constant jerk motion [16]. Jerk, acceleration and velocity limits: J, A, V.

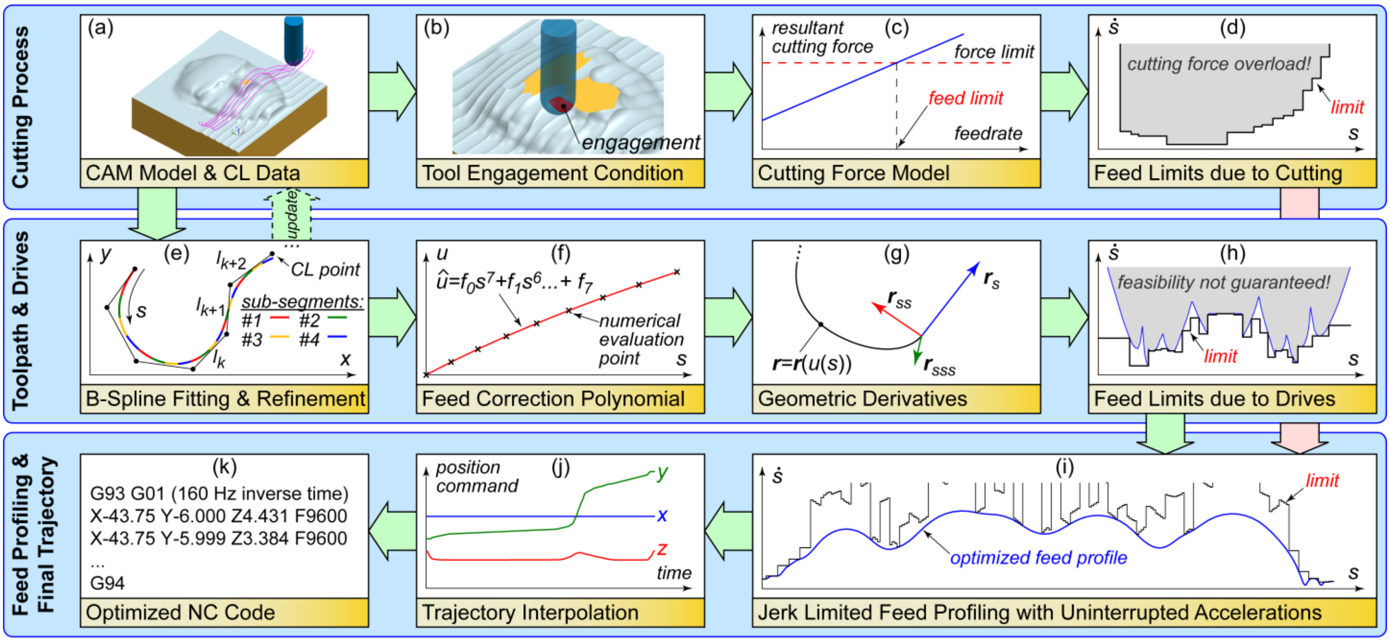


**Fig. 6.** Overall feedrate optimization scheme.

predict cutting forces. By simulating forces for the toolpath at two different constant feeds, the relationship between feedrate and the resultant cutting force is determined for the individual cutter locations (Fig. 6c). This is used to determine the local feed limit, imposed by the cutting process (Fig. 6d), as a function of tool progression (i.e., arc displacement ( $s$ )) along the toolpath.

The CL points are smoothened into $C^2$ toolpaths by fitting cubic B-splines (Fig. 6e) [17]; which are efficiently parameterized considering four successive points at a time. Then, the B-spline toolpaths are converted into cubic polynomials, which are suitable for interpolation. B-spline parameterization ensures that unwanted geometric fluctuation does not occur, due to its 'convex hull' property. Each toolpath segment is then divided (illustrated as #1, #2, #3, and #4 in Fig. 6e), to allow less conservative setting of feed limits, which depend on the local geometric derivatives.

Since spline arc lengths are not known ahead of time, the B-splines are parameterized using the average chord length ( $0 \le u \le U_k$ ), computed by taking the mean of three consecutive chord lengths ( $U_k = (l_k + l_{k+1} + l_{k+2})/3$ ). After the toolpath is parameterized, the actual arc length ( $s$ ) is integrated numerically, by applying Simpson's rule. Numerical evaluation points computed during integration also help to characterize the relationship between the spline parameter ( $u$ ) and actual arc displacement ( $s$ ). This is approximated with a feed correction polynomial [18], as shown in Fig. 6f. This polynomial allows the spline toolpath $\boldsymbol{r} = \boldsymbol{r}(u)$ to be interpolated with the desired arc displacement $\boldsymbol{r} = \boldsymbol{r}(\hat{u}(s))$ , thereby eliminating unwanted feedrate fluctuation, or discontinuity at segment connections. The feed correction polynomial also allows calculation of the geometric derivatives of tool position with respect to the arc parameter, shown in Fig. 6g, using the chain rule:

$$\boldsymbol{r}_s = \boldsymbol{r}_u u_s \; , \; \boldsymbol{r}_{ss} = \boldsymbol{r}_{uu} u_s^2 + \boldsymbol{r}_u u_{ss}$$
$$\boldsymbol{r}_{sss} = \boldsymbol{r}_{uuu} u_s^3 + 3\boldsymbol{r}_{uu} u_s u_{ss} + \boldsymbol{r}_u u_{sss} \tag{6}$$

These derivatives are used to compute the local feed limit due to drive constraints, shown in Fig. 6h, using Eqs. (4)-(5). In Fig. 6i, the optimized feed profile $s = s(t)$ is generated by simultaneously considering the feed limits imposed by the cutting process and feed drives. The profiling algorithm brings the commanded feed as close as possible to the local limits, while guaranteeing a final full stop with kinematic compatibility from the initial state. The profile adheres to the specified tangential acceleration ( $a$ ) and jerk ( $J$ ) magnitudes, and unnecessary zero crossings of the tangential acceleration are avoided at segment boundaries. This enables smoother motion, yielding shorter cycle time, compared to using piece-wise constant feed modulation with smooth acceleration transitions in between, as applied in [8][10]. Details of the feed profiling algorithm can be found in [19].

Once the toolpath and feed profile are parameterized, they are interpolated together to generate time dependent position commands at a certain sampling frequency, which can be programmed into the NC code in 'inverse-time' feed mode (Fig. 6j-Fig. 6k). This frequency was chosen as 160 Hz, which is near the upper programming limit allowed by the Fanuc 30i controller.

In the current state of implementation, the original CL data is used both in cutting force prediction and B-spline fitting. This can lead to some discrepancy between the predicted and actual cutting forces. This is attributed to the lack of sufficiently close CL points generated by the CAM software, and minor changes in the toolpath caused by B-spline fitting. Next stage of implementation targets using the fitted spline toolpath in the force prediction steps, for better data resolution and prediction accuracy, as indicated with the 'update' arrow connecting Fig. 6e to Fig. 6a.

## 5. Experimental results

The proposed strategy was validated in optimizing the roughing layer for sculptured surface. The workpiece is Al-7050 and the tool is a 6 mm radius ball end mill. The toolpath was generated with 0.04 mm tolerance, leading to 11,186 CL points for the complete operation. Processing by the solid modeler, applying the B-rep method, took 482 s and consumed 1.2 GByte of memory. In feed planning, the resultant force limit was set to 200 N. A Mori Seiki NMV 5000DCG machining center was used in the cutting tests. The drives' velocity, acceleration, and jerk limits were identified by inspecting the corresponding registers in the CNC.

The workpiece and toolpaths are shown in Fig. 7a-b. The kinematic profiles for a sample pass (#5) are shown in Fig. 7c. As can be seen, the optimized feed profile closely follows the feed

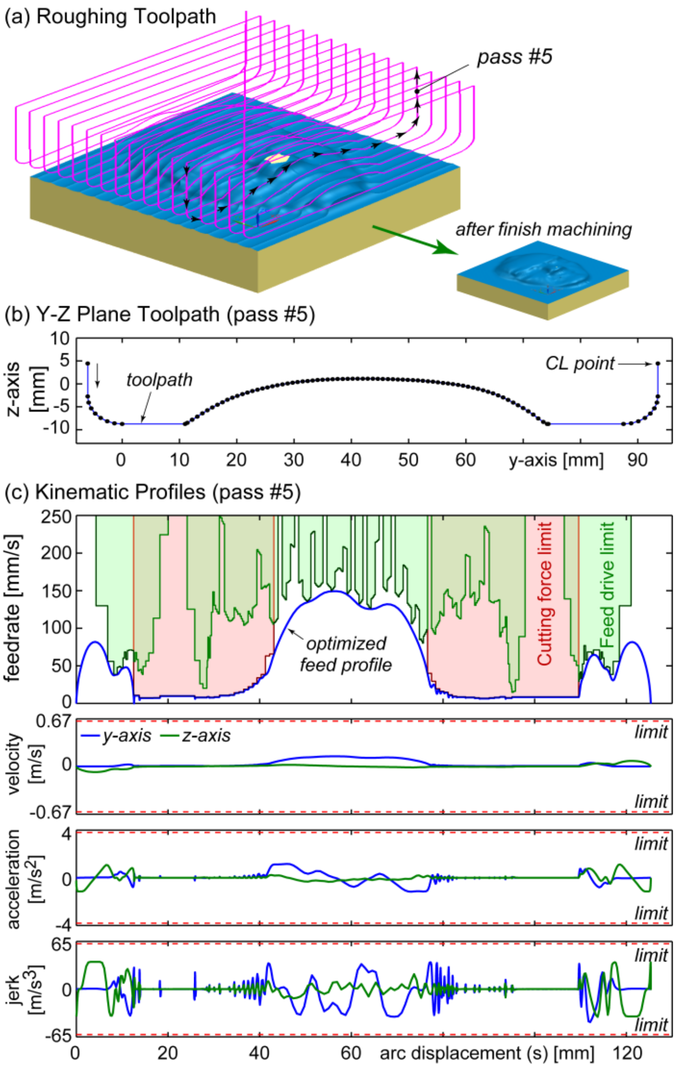


**Fig. 7.** Roughing toolpath and kinematic profiles for a sample pass.

limits set by the cutting process and drives. When the process is dominant, smaller feeds are commanded. During air cutting, in mid-pass, drive limits become dominant and higher feeds are commanded. The velocity, acceleration, and jerk bounds are never exceeded, and the jerk capability of the y-axis is reasonably well utilized. However, the limit is (usually) not reached, due to the mentioned conservativeness in solving $f_k$ from Eq. (4). A less conservative approach is also currently under development.

The machined part and measured cutting forces are shown in Fig. 8 and Fig. 9. The machining cycle time is compared to the case of using only constant feed to achieve the same force limit. As can be seen, by applying the presented optimization scheme, the overall cycle time for the 17-pass toolpath is reduced by 16%. Owing to the roughing nature of the operation, the cutting process is dominant in determining the cycle time. In finishing


**Fig. 8.** Roughing layer of sculptured surface.

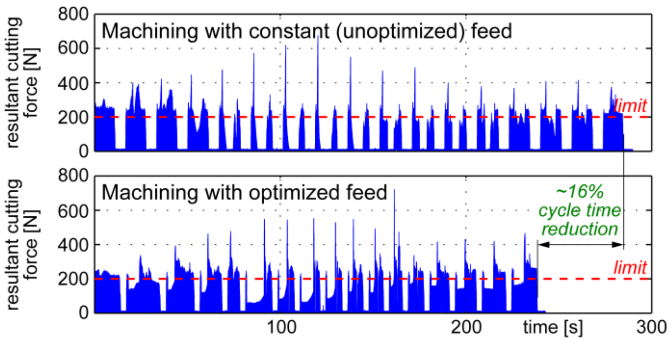


**Fig. 9.** Resultant cutting forces and cycle time comparison.

operations, different results are expected; where both factors, the process and the drives, may play similarly important roles.

## 6. Conclusions

This paper has presented a novel and comprehensive strategy for planning minimum cycle time tool trajectories, subject to both machining process and machine tool drive limits. The implementation has been experimentally validated in rough machining of a sculptured surface. Impact of this methodology on finishing operations is currently under investigation.

## Acknowledgments

The authors acknowledge the Machine Tool Technologies Research Foundation (MTTRF), Mori Seiki Co., and Turkish Aerospace Industry Inc., for their support to Koç University.

## References

[1] Budak, E., Lazoglu, I., Guzel, B.U., 2004, Improving Cycle Time in Sculptured Surface Machining Through Force Modeling, Annals of the CIRP, 53/1:103-106.
[2] Erdim, H., Lazoglu, I., Ozturk, B., 2006, Feedrate Scheduling Strategies for Free-Form Surfaces, Int. J. Mach. Tool. & Manuf., 46:747–757.
[3] Tunc, L., Budak, E., 2009, Extraction of 5-Axis Milling Conditions from CAM Data for Process Simulation, Int. J. Adv. Manuf. Tech., 43:538-550.
[4] Lazoglu, I., Boz, Y., Erdim, H., 2011, Five-Axis Milling Mechanics for Complex Free From Machining, Annals of the CIRP, 60/1:117-120.
[5] Koninckx, B., Van Brussel, H., 2002, Real-Time NURBS Interpolator for Distributed Motion Control, Annals of the CIRP, 51/1:315-318.
[6] Brecher, C., Lange, S., Merz, M., Niehaus, F., Wenzel, C., Winterschladen, M., Weck, M., 2006, NURBS Based Ultra-Precision Free-Form Machining, Annals of the CIRP, 55/1:547-550.
[7] Heng M., Erkorkmaz K., 2010, Design of a NURBS Interpolator with Minimal Feed Fluctuation and Continuous Feed Modulation Capability", Int. J. Mach. Tool. & Manuf., 50:281–293.
[8] Weck, M., Meylahn, A., Hardebusch, C., 1999, Innovative Algorithms for Spline-Based CNC Controller, Annals of the German Academic Society for Production Engineering, VI/1:83-86.
[9] Altintas, Y., Erkorkmaz, K., 2003, Feedrate Optimization for Spline Interpolation in High Speed Machine Tools, Annals of the CIRP, 52/1:297-302.
[10] Erkorkmaz, K., Heng, M., 2008, A Heuristic Feedrate Optimization Strategy for NURBS Toolpaths", Annals of the CIRP, 57/1:407-410.
[11] Sencer, B., Altintas, Y., Croft, E., 2008, Feed Optimization for Five-Axis CNC Machine Tools with Drive Constraints, Intl. J. Mach. Tool. & Manuf., 48:733–745.
[12] Lee, H.U., Cho, D.W., 2003, An Intelligent Feedrate Scheduling Based on Virtual Machining, Int. J. Adv. Manuf. Tech., 22:873–882.
[13] Altintas, Y., Merdol, D.S., 2007, Virtual High Performance Milling, Annals of the CIRP, 55/1:81-84.
[14] Merdol, D.S., Altintas, Y., 2008, Virtual Cutting and Optimization of Three-Axis Milling Processes, Int. J. Mach. Tool. & Manuf., 48:1063-1071.
[15] Merdol, D.S., 2008, Virtual Three-Axis Milling Process Simulation and Optimization, Ph.D. Thesis, University of British Columbia, Vancouver.
[16] Altintas, Y., 2012, Manufacturing Automation: Metal Cutting Mechanics, Machine Tool Vibrations and CNC Design – 2nd Ed., Cambridge University Press.
[17] Piegl, L., Tiller, W., 2003, The NURBS Book - 2nd Edition, Springer-Verlag, 2003.
[18] Erkorkmaz, K., Altintas, Y., 2005, Quintic Spline Interpolation with Minimal Feed Fluctuation, ASME J. Manuf. Sci. & Eng., 127/2:339-349.
[19] Erkorkmaz, K., 2012, Real-Time Feed Optimization for Spline Toolpaths Employing Uninterrupted Acceleration Profiling, Proc. 27th ASPE Annual Mtg., San Diego, CA, Oct 21-26.